

Neutral Atoms Behave Much Like Classical Spherical Capacitors

James C. Ellenbogen*

Nanosystems Group, The MITRE Corporation, McLean, Virginia 22102, USA

(Dated: September 25, 2006; submitted for publication January 3, 2006)

The scaling of the capacitance with radius is explored in detail for neutral atoms, and it is found that they behave much like macroscopic spherical capacitors. The quantum capacitances of atoms scale as a linear function of the mean radii of their highest occupied orbitals. The slopes of the linear scaling lines include a dimensionless constant of proportionality κ that is somewhat analogous to a dielectric constant, but for individual atoms. The slope and κ assume discrete values characteristic of elements in different regions of the periodic table. These observations provide a different, electrostatics-based way of understanding the periodic behavior of the elements.

PACS numbers: 31.10.+z, 03.65.Sq, 31.25.-v, 31.90.+s

I. INTRODUCTION

There is widely perceived to be a dichotomy between the classical behavior [1] of macroscopic electrical devices and quantum behavior [2, 3] in the electrical properties of atoms and molecules on the picometer and nanometer scales. Here, however, we report on unexpected quasi-classical regularities found in the electrical behavior of neutral atoms. Specifically, we explore the variation or “scaling” of the quantum capacitances for neutral atoms as a function of the mean radii for their outermost orbitals. This quantum scaling behavior for atoms is seen to resemble strongly the linear capacitance scaling behavior of macroscopic spherical conductors in classical electrostatics.

These linear, quasi-classical regularities in the quantum behavior of atoms provide a different, electrostatics-based way of understanding the periodic behavior of the elements. Also, the linear capacitance scaling relations for atoms can be shown to establish a particularly simple quantitative relationship between an atom’s valence electron detachment energies and its dimensions (i.e., the mean radius for its outermost orbital).

The generally linear nature of capacitance scaling for neutral atoms has been noted previously by Gazquez and Ortiz [4], by Komorowski [5], and by Perdew [6]. However, here we explore the scaling using a different measure of the atomic radius than prior investigators, and unexpected details emerge as a result.

Figure 1 plots experimentally derived atomic capacitances versus the *ab initio* mean radii $\langle r \rangle_a$ of the highest energy or “outermost” occupied atomic orbitals for 24 representative atoms. This plot reveals an unanticipated variety of linear behaviors. Different classes of elements fall on different lines, but some lines have the same or nearly the same slope. Contrary to one’s initial expectations from the scaling of isolated spheres in classical electrostatics [1], for isolated atoms the capacitance scaling lines extrapolate to nonzero intercepts C_0 with the

capacitance axis. As with the slopes, there are fewer values of C_0 than there are scaling lines. The few discrete ranges of values for the slopes and intercepts may be associated with the different angular momentum states (*S* and *P* states) of the atoms plotted along the lines.

II. METHOD AND RESULTS

In this work, we follow Froese-Fisher [7] in employing as a measure of the atomic radius the mean radius $\langle r \rangle_a$ associated with the highest occupied Hartree-Fock atomic orbital $\phi_a(r)$, where $a=N$ for an N -electron atom. Defining the electron density component $\rho_a(r) = |\phi_a(r)|^2$,

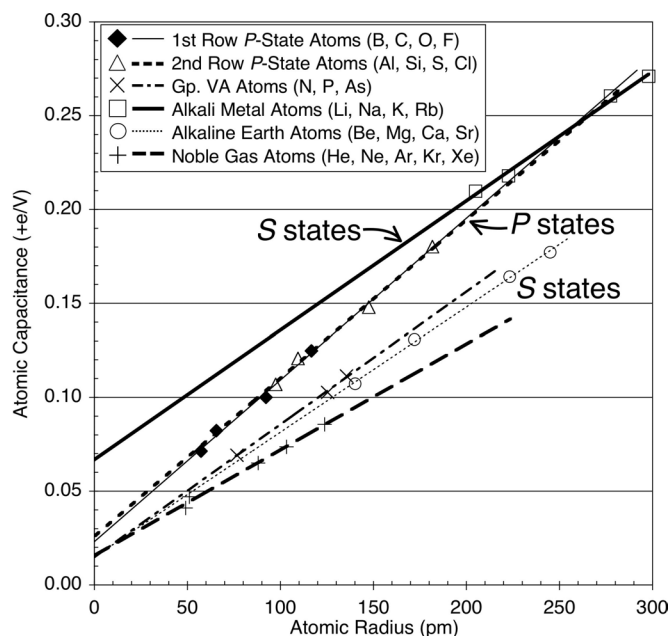


FIG. 1: Atomic Capacitance Scaling versus Mean Radius. Atomic capacitances C_I in fundamental units of positive charge per Volt ($+e/V$), from Table I, are plotted vs. mean radii $\langle r \rangle_a$ for the atoms’ highest occupied Hartree-Fock orbitals, as given by Froese-Fisher [7, 8]. Lines are fit to points via linear regression, with fitting parameters listed in Table I.

*Electronic address: ellenbgn@mitre.org

TABLE I: Accurate Atomic Capacitances and Atomic Radii. Capacitances C_I in fundamental positive charges per Volt ($+e/V$) for 24 neutral atoms are reported as a function of the mean radii [7, 8] $\langle r \rangle_a$ of their highest occupied Hartree-Fock (HOHF) orbitals. C_I was calculated using Eq. (1), based upon experimental ionization potentials (I 's) and electron affinities (A 's) for the atoms [9–11], except as noted. Radii $\langle r \rangle_{a+1}$ for the anions' HOHF orbitals were calculated by the author from Clementi-Roetti [12] anion orbitals, for species where they are given. Dashes signify that a quantity is not known with accuracy. With $+e/V$ as the unit for capacitance and pm for length, the permittivity of free space is $\epsilon_0 = 5.526349 \times 10^{-5} +e/V\text{-pm}$.

Group in Periodic Table	Neutral Atom		Anion		I (eV)	A (eV)	C_I ($+e/V$)	Approx. C_I if $ A $ v. small, $1/I$	Linear Regression Parameters for Plots of C_I vs. $\langle r \rangle_a$			Dielectric Constant, $\frac{\text{Slope}}{4\pi\epsilon_0} = \kappa$	Angular Momentum Term Symbol
	No., Z	Atom	Radius $\langle r \rangle_a$ (pm)	Radius $\langle r \rangle_{a+1}$ (pm)					Slope	Intercept, C_0	R^2		
1st Row	5	B	117	193	8.30	0.280	0.125						
P-States	6	C	92	114	11.26	1.262	0.100		8.61	0.0231	0.990	1.24	P
	8	O	66	79	13.62	1.461	0.082		$\times 10^{-4}$				
	9	F	57	66	17.42	3.401	0.071						
2nd Row	13	Al	182	241	5.99	0.433	0.180						
P-States	14	Si	148	171	8.15	1.390	0.148		8.43	0.0259	0.995	1.21	P
	16	S	110	123	10.36	2.077	0.121		$\times 10^{-4}$				
	17	Cl	98	107	12.97	3.613	0.107						
VA	7	N	75	93	14.53	-0.07	0.07						
	15	P	123	144	10.49	0.75	0.10		7.13	0.0159	0.999	1.03	$^4S_{3/2}$
	33	As	133	154	9.79	0.81	0.11		$\times 10^{-4}$				
IA: Alkali Metals	3	Li	205	304	5.39	0.618	0.210						
	11	Na	223	320	5.14	0.548	0.218		6.89	0.0668	0.994	0.99	$^2S_{1/2}$
	19	K	277	394	4.34	0.501	0.260		$\times 10^{-4}$				
	37	Rb	298	389	4.18	0.486	0.271						
IIA: Alkaline Earths	4	Be	140	-	9.32	-	-	0.107					
	12	Mg	172	-	7.65	-	-	0.131	6.66	0.0149	0.999	0.97	1S_0
	20	Ca	223	-	6.11	0.024	0.164	0.164	$\times 10^{-4}$				
	38	Sr	245	-	5.69	0.052	0.180	0.177					
VIII: Noble Gases	2	He	49	-	24.59	-0.22 ^a	0.040						
	10	Ne	51	-	21.57	-0.30 ^a	0.046						
	18	Ar	88	-	15.76	-0.37 ^a	0.062		5.63	0.0157	0.991	0.81	1S_0
	36	Kr	103	-	14.00	-0.42 ^a	0.069		$\times 10^{-4}$				
	54	Xe	124	-	12.13	-0.45 ^a	0.079						

^aNegative A extrapolated from experiment [13] by Zollweg [14].

the mean radius is calculated $\langle r \rangle_a = \int_0^\infty r \rho_a(r) 4\pi r^2 dr$. Canonical tables [8, 12, 15] are available of the *ab initio* Hartree-Fock atomic orbitals, as well as of their mean radii, and these tables were used in this work.

To evaluate the atomic capacitances given in Table I and plotted in Fig. 1, we use a formula for quantum systems due to Iafrate *et al.* [16] and to Perdew [6]:

$$C_I = 1/(I - A). \quad (1)$$

This equation evaluates the capacitance for an N -electron quantum system with total energy $E(N)$ having a first ionization potential $I = E(N - 1) - E(N)$ and an electron affinity $A = E(N) - E(N + 1)$. Here, the N -electron system is the lowest energy neutral state. Its A is negative if its anion is not stable with respect to the N -electron state, as for the Ne atom, for example.

Equation (1) differs from the one written by Iafrate *et al.* by a factor of $1/e^2$. This unit transformation assumes that the I 's and A 's are expressed in eV, the unit commonly used in tabulations [10, 11] of atomic and molecular electron detachment energies. Thus, Eq. (1) yields

the capacitances in atomic-scale units of fundamental positive charges per Volt (which we symbolize here as “ $+e/V$ ”).

Equation (1) is applied to calculate C_I for 24 atoms from experimentally determined [9–11, 13, 14] I 's and A 's for their neutral states. These detachment energies and the resulting values of C_I are presented in Table I. For Be and Mg, it appears from a search of the literature that there are no generally accepted values of the A 's, which are thought to be negative [9] and probably are small in magnitude. For those two atoms only, therefore, we use $C_I \approx 1/I$. This approximation is tested in column 9 of the table and seen not to affect significantly values of C_I for the next two atoms in the same column of the periodic table, for which A 's are known, but also small.

In Fig. 1, each of the 24 values determined for C_I is plotted versus the corresponding value of $\langle r \rangle_a$, as determined in atomic Hartree-Fock calculations [7, 8]. Several regression lines also are plotted for the $(\langle r \rangle_a, C_I)$ points. The regression parameters are given in columns 10 through 12 of Table I.

The atoms reported upon here were chosen as a result of several steps in the research. Initially, C_I was determined and plotted versus $\langle r \rangle_a$ for all of the atoms with atomic numbers $Z=2$ to 18. Then, from inspection of a C_I versus $\langle r \rangle_a$ plot that was the precursor of Fig. 1, it was determined that most of the atoms fell on two, nearly overlapping regression lines. These are the two labeled in Fig. 1 as representing P states. However, some atoms—esp., Be and Mg, N and P, as well as Ne and Ar—generated points off those two lines, which are associated with the filling of the $2p$ and $3p$ orbitals, respectively.

This led to the determination and plotting of the $(\langle r \rangle_a, C_I)$ points for more atoms from each of the columns on the periodic table—IIA, VA, and VIII—associated with points that fell off the main lines. Points for atoms from each of these columns then were seen to form lines of their own, as shown in Fig. 1. Shortly, it was recognized that all these atoms that were off the two primary overlapping regression lines shared the characteristic that they were S states. By contrast, most of the atoms then remaining on the primary lines were P states.

The points for S -state atoms Li and Na actually could be fit quite satisfactorily on regression lines for the first and second row P -state atoms. However, with the realization that slopes for the lines depend strongly upon the total angular momentum quantum number L of the associated atoms, the S -state ($L=0$) atoms Li and Na, along with points added for K and Rb, were grouped separately from the P -state ($L=1$) atoms. Then, a regression line also was determined for these four Group IA atoms, as seen in Fig. 1. As shown in Table I, all six regression lines fit their respective data points with large R^2 values, indicating exceptionally strong linear correlations between the atomic capacitances and atomic radii.

III. ANALYSIS

Any analysis of the atomic capacitance scaling results presented above must begin by remarking how much they resemble the results that would be expected if atoms simply were conducting spheres subject to the laws of classical electrostatics. The atoms seem to obey an analog of the elementary classical equation [1]

$$C = 4\pi\epsilon_0\kappa r_a [1 - (r_a/r_{a+1})]^{-1} \quad (2a)$$

$$\approx 4\pi\epsilon_0\kappa r_a, \text{ if } r_{a+1} \gg r_a. \quad (2b)$$

$$\approx 4\pi\epsilon_0\kappa r_a + 4\pi\epsilon_0\kappa[(r_a)^2/r_{a+1} + \dots], \text{ if } r_{a+1} \gtrsim r_a. \quad (2c)$$

This describes the capacitance C of a classical spherical conductor of radius r_a that is positioned within a larger, concentric spherical conductor of radius r_{a+1} . The parameter κ is the dielectric constant of the intervening medium and ϵ_0 is the permittivity of free space.

For the atom or “atomic capacitor” with quantum capacitance C_I , an analog of the classical inner conductor is the charge density $\rho_a(r)$, having mean radius $\langle r \rangle_a$. An

analog of the classical outer conductor is the charge density $\rho_{a+1} = |\phi_{a+1}|^2$ for the highest occupied orbital ϕ_{a+1} on the atomic anion, with mean radius $\langle r \rangle_{a+1}$. Then, the energy $(I-A)$ in Eq. (1) is approximately that for an electron on the neutral atom to undergo an $a \rightarrow a+1$ transition. This places a charge $-e$ on outer conductor ρ_{a+1} and leaves a “hole” with charge $+e$ on inner conductor ρ_a , with potential $V = (I-A)/e$ having been applied to separate the charges. This separation includes adjustment in $\rho^{(N-1)}$, the density for the atom’s other $N-1$ electrons. The analog of the dielectric in this atomic capacitor model is the portion of the new $\rho^{(N-1)}$ that “screens” the positive and negative charges in ρ_a and ρ_{a+1} from each other.

We observe above that the $(\langle r \rangle_a, C_I)$ points for the atoms produce excellent fits to regression equations that may be stated in a form analogous to the classical Eq. (2):

$$C_I = 4\pi\epsilon_0\kappa\langle r \rangle_a + C_0. \quad (3)$$

As above, C_0 is the capacitance intercept at $\langle r \rangle_a = 0$. Its nonzero values have no analog in the classical Eq. (2b) for an isolated spherical conductor. The nonzero intercept does have an analog, though, in the equations for a classical spherical capacitor if r_{a+1} is not very much larger than r_a , as in Eq. (2c), and if the sum there in square brackets is nearly linear or constant in r_a .

Such behaviors also are exhibited by several groups of atoms and might help account for the atoms’ nonzero C_0 , by analogy with Eq. (2c). From above, even on an isolated atom, ρ_{a+1} acts like an outer conductive sphere for ρ_a . Also, $\langle r \rangle_{a+1}$ is not very much larger than $\langle r \rangle_a$, while $[(\langle r \rangle_a)^2/\langle r \rangle_{a+1}]$ is nearly linear in $\langle r \rangle_a$, at least for the first four groups of atoms in Table I, as may be verified from atom and anion radius data given there.

In Eq. (3), to emphasize the analogy to classical Eqs. (2), we write $4\pi\epsilon_0\kappa$ for the slope of the atomic capacitance scaling line, thereby defining a dimensionless constant of proportionality κ that acts somewhat like a dielectric constant for an atom. Then, for any atom along the line $\kappa = \text{Slope}/4\pi\epsilon_0$. Via this relation, κ is calculated from the slopes of the regression lines for all six groups of atoms and reported in column 13 of Table I. These dielectric constants fall into three discrete sets: (1) P states having $\kappa \approx 1.2$, (2) most of the S states with $\kappa \approx 1$, and (3) the noble gas atoms (also S states) with $\kappa = 0.81$.

From Table I, the anomalously small value of κ for noble gas S -state atoms arises partly because their I ’s fall off less rapidly with increasing Z (and increasing principal quantum number for the valence electron) than do I ’s for other sequences of S -state atoms (cf. Group IIA). This leads C_I to grow more slowly for noble gas atoms as they get larger. Also, though these atoms tend to be smaller than the other S -state atoms, their radii grow more rapidly with increasing valence principal quantum number. Thus, $\kappa \sim (\Delta C/\Delta\langle r \rangle_a)$ is unusually small.

The large I ’s and small size of the noble gas atoms are due to their completely filled valence shells. This makes it hard to add charge to them or to polarize their electrons.

In classical electrostatics, such systems are said to have low capacitances and small dielectric constants, just as these atoms are seen to have here.

In Fig. 1, because regression lines with different slopes or dielectric constants fit points for groups of atoms from different parts of the periodic table, one might say that the valence dielectric constant of an atom is a new characteristic periodic property of the elements. The very strong correlation of the atomic capacitances, κ , and C_0 with the periodic table is evident if one compares the lines in the figure to the columns on a periodic table. The two bounding, upper and lower lines correspond to the two bounding columns (the alkali metals and noble gases, respectively) at opposite ends of the periodic table. Other lines that connect these extreme lines correspond to elements in rows that analogously connect the extreme columns of the periodic table.

The accuracy of Eq. (3) in fitting values from Eq. (1) suggests one may eliminate C_I between Eqs. (1) and (3). Then, after slight rearrangement, one obtains:

$$A = I - \frac{1}{4\pi\epsilon_0 \kappa \langle r \rangle_a + C_0}. \quad (4)$$

This quantum equation shows a previously unappreciated relationship among the valence electron detachment energies and the mean dimensions of a many-electron atom. In Eq. (4), the atomic dielectric constant modulates a constraint that determines some of the periodic properties of an atom (e.g., the usually difficult-to-obtain electron affinities A) in terms of others (e.g., the easier-to-obtain ionization potentials I and mean radii). Equation (4) also provides a new explanation for the relative magnitudes and signs of the electron affinities. As an atom's radius gets smaller, the absolute magnitude of the second term on the right-hand side of the equation gets large and the term makes an increasingly negative contribution to A . This produces a smaller value of A for the atom. A small dielectric constant amplifies this

effect, while a large one mitigates it.

If $\langle r \rangle_a$ is small enough, though, the second term on the right becomes larger in absolute magnitude than I , and a negative A results. A physical interpretation of this, rooted in the analogy with classical electrostatics, is that atoms like Be, N, or the noble gas atoms, with relatively small dielectric constants *and* small mean radii, do not have sufficiently polarizable electrons in the valence region, nor sufficient surface area on which to distribute an additional electron to produce a stable anion.

In summary, it has been demonstrated in this paper that the scaling of the quantum capacitances of atoms with their mean radii exhibits quasi-classical regularities. Further, it has been shown that this scaling yields a different qualitative perspective and quantitative perspective, via Eq. (4), on the periodic behavior of the elements. Equation (4), together with the similarity in form of Eq. (3) for atomic capacitors to Eqs. (2) for classical capacitors, also suggests a different, simple interpretation for the quantum structure of atoms. This interpretation is based upon an analogy with classical electrostatics, rather than upon the usual analogy [2, 3] with classical mechanics. This electrostatics-like approach to explaining quantum behavior is to be explored further for both atoms and molecules in several subsequent publications.

Acknowledgments

The author gratefully acknowledges valuable conversations with C. Picconatto, J. Burnim, S. Das, M. Halper, and E. Shamir of the MITRE Nanosystems Group. He thanks D. Goldhaber-Gordon of Stanford U. for helpful comments on the manuscript. The author also is very appreciative of the encouragement of this and related work over a number of years by leaders at the MITRE Corporation. This research was supported by the MITRE Technology Program.

-
- [1] D. Halliday, R. Resnick, and J. Walker, *Fundamentals of Physics* (Wiley, New York, NY, 2001), sixth ed.
- [2] L. Pauling and E. B. Wilson, *Introduction to Quantum Mechanics with Applications to Chemistry* (McGraw-Hill, New York, 1935), republished by Dover, NY, 1985.
- [3] M. Karplus and R. N. Porter, *Atoms and Molecules* (Addison-Wesley, New York, NY, 1970).
- [4] J. L. Gazquez and E. Ortiz, *J. Chem. Phys.* **81**, 2741 (1984).
- [5] L. Komorowski, *Chem. Phys. Lett.* **134**, 536 (1987).
- [6] J. P. Perdew, *Phys. Rev. B* **37**, 6175 (1988).
- [7] C. Froese, *J. Chem. Phys.* **45**, 1417 (1966).
- [8] C. Froese-Fisher, *The Hartree-Fock Method for Atoms: A Numerical Approach* (Wiley, New York, NY, 1977).
- [9] T. Andersen, H. Haugen, and H. Hotop, *J. Phys. Chem. Ref. Data* **28**, 1511 (1999).
- [10] D. R. Lide, ed., *Handbook of Chemistry and Physics* (CRC Press, Boca Raton, FL, 2004), 85th ed., see esp. Tables of I 's and A 's in Section 10.
- [11] P. J. Lindstrom and W. G. Mallard, eds., *NIST Chemistry WebBook*, NIST Standard Reference Database No. 69 (Natl. Inst. of Standards and Technology, 2005), <http://webbook.nist.gov/chemistry/>.
- [12] E. Clementi and C. Roetti, *At. Data Nucl. Data Tables* **14**, 177 (1974).
- [13] C. E. Kuyatt, J. A. Simpson, and S. R. Mielczarek, *Phys. Rev.* **138**, A385 (1965).
- [14] R. J. Zollweg, *J. Chem. Phys.* **50**, 4251 (1969).
- [15] C. F. Bunge and J. A. Barrientos, *At. Data Nucl. Data Tables* **53**, 113 (1992).
- [16] G. J. Iafrate, K. Hess, J. B. Krieger, and M. Macucci, *Phys. Rev. B* **52**, 10737 (1995).

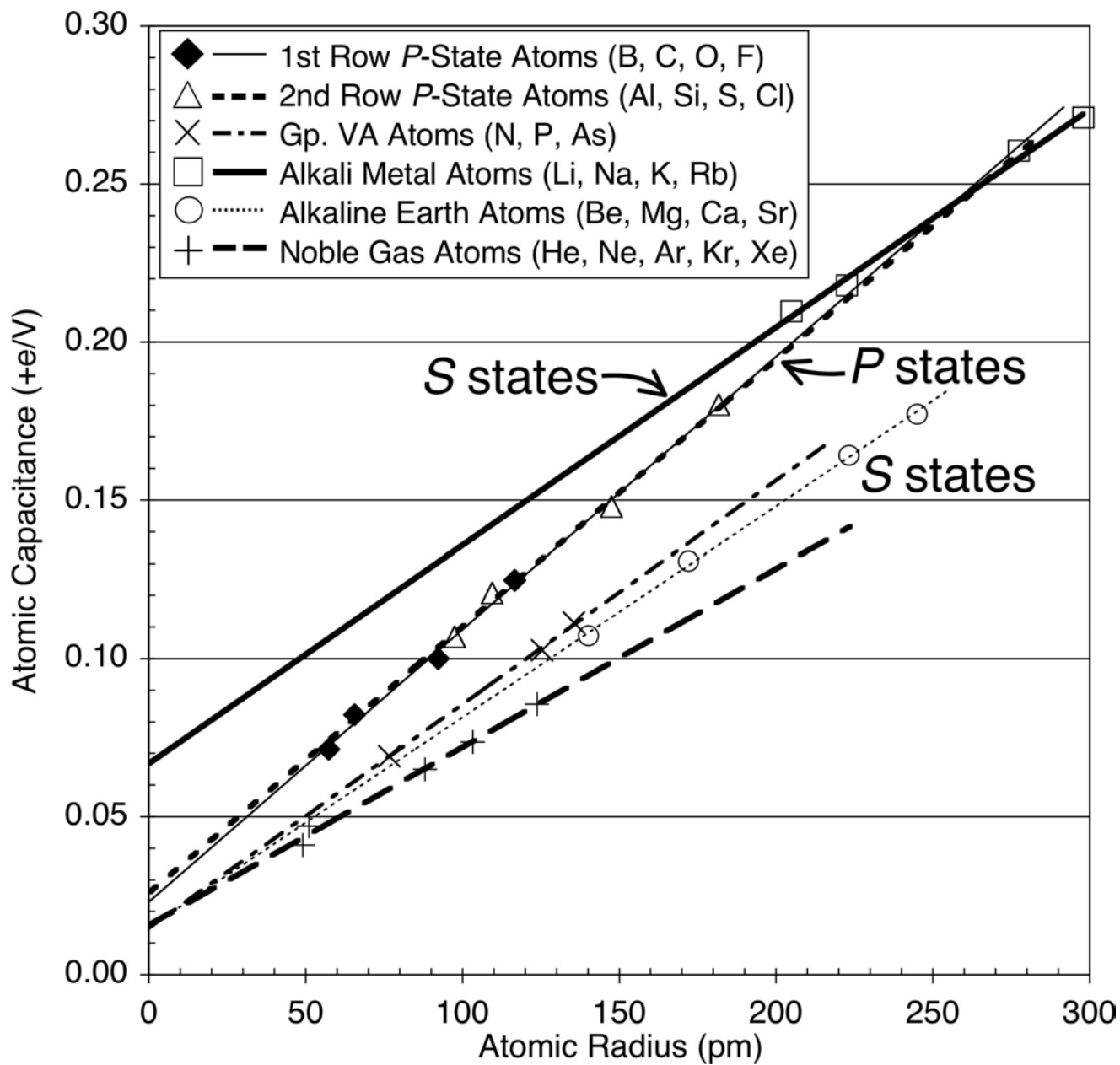


Figure 1